SEMARAK ILMU PUBLISHING

Journal of Advanced Research in Fluid Mechanics and Thermal Sciences

Journal homepage:
https://semarakilmu.com.my/journals/index.php/fluid_mechanics_thermal_sciences/index
ISSN: 2811-3950

Fluid Viscosity Measuring Instrument with Internet of Things (IoT) Based Rotary Method

Herry Sufyan Hadi[1,*], Putri Yeni Aisyah[1], Syamsul Arifin[1], Ahmad Fauzan Adziimaa[1], Arief Abdurrakhman[1]

[1] Instrumentation Engineering Department, Vocational Faculty, Sepuluh Nopember Institute of Technology (ITS) Surabaya, East Java, Indonesia

ARTICLE INFO

Article history:
Received 26 September 2021
Received in revised form 11 December 2021
Accepted 21 December 2021
Available online 31 January 2022

Keywords:
Viscometer; Rotary Method; Simulink Matlab; Monitoring; IoT

ABSTRACT

The viscometer is a system measuring the viscosity value of a liquid substance. The function of this viscosity measuring instrument is used to analyze the viscosity level of a particular product so that it is easy to know the quality of fluid viscosity. In this research, two methods were conducted, namely simulation and experimentation. Simulations were conducted using Simulink Matlab while experiments were conducted by designing fluid viscosity measuring instruments by rotary method or commonly known as a rotational viscometer. This tool uses two sensors namely, rpm sensor to measure rpm of dc motor and current and voltage sensor to measure current from dc motor, and also use controller equipped with Internet of Things (IoT) so that the measurement results will be displayed through LCD and can be monitored through the website. From the simulation results obtained drum motor spinning at low speed to the 10th second of the motor rotation about 6 rad / s and as time increases, the motor rotation will increase until the 60th second of the motor rotation begins to be constant this is due to the large shear voltage produced by a fluid at the beginning of the motor is turned on very large and decreases over time. While the test results of the tool that has been designed, obtained the measurement results on SAE 40 Oil obtained accuracy results of 0.99, on the measurement of SAE Oil 20W-50 obtained an accuracy value of 0.99 and in the measurement of SAE 10W-30 Oil obtained an accuracy value of 0.99.

1. Introduction

One of the measuring instruments needed in the industrial world is the viscometer. The viscometer is a system of viscosity value gauge (viscosity) of a liquid substance [1]. The function of this viscosity measuring instrument is used to analyze the viscosity level of a particular product so that it is easy to know the quality of fluid viscosity. Examples of industries that require viscometers are industries that produce products in the form of liquids such as lubricants, oil processing, paints, chemicals, etc.

Viscosity is a measure of the viscosity of liquid substances. Viscosity values are indispensable in determining the physical properties of liquids. Because viscosity value affects a product to be

* *Corresponding author.*
E-mail address: sh_herry@yahoo.co.id

https://doi.org/10.37934/arfmts.92.1.6589

produced. For example, in the food production process, if the viscosity value in food is high it will refer to the flour and glucose substances present in the food [2]. The second example is in vehicle lubricants, in-cylinder temperature vehicles, gears, and driving engines can be affected by oil viscosity. In addition, friction in the engine is also affected by oil viscosity [2]. The third example is in the field of health, viscosity is also needed in the field of health to measure blood viscosity affected by plasma viscosity and hematocrit with viscosity can be detected in various diseases for example in patients who have an acute cardiovascular disease such as stroke and heart attack, plasma viscosity will be higher. In addition, anemia, postmenopausal epidemic [2]. The fourth example is in the manufacturing industry, viscosity plays a role in the measurement of the viscosity of lubricants to be used in the machine. If the lubricant has a too high viscosity, then the lubricant can clog the machine thus hindering the manufacturing process [2]. Liquids with high viscosity values are more difficult to flow compared to liquids that have low viscosity [3]. Conventionally, viscosity measurement has insufficient precision for that it is necessary to use a measuring instrument that is easy to use and has better precision [3]. There are several methods to measure viscosity values such as falling ball viscometer, rotational viscometer, and capillary tube viscometer. The one-axis cylinder rotation type viscometer is based on 2 types of Searle system and Couette system. On Searle systems, the inner cylinder rotates and the outer cylinder is stationary. The opposite of the Searle system, on the Couette system the outside of the cylinder is rotated while the inside of the cylinder is still [3]. Viscosity of reference oils was measured both with the Brookfield type viscometer and with the rheometer at 20°C and at the same angular velocity range. Uncertainty of measurement was calculated and results were compared with reference values [13]. The viscometer of a falling ball is a viscosity measuring instrument that measures the time a ball passes through a liquid at a certain distance based on the principles of Stokes Law and Newton's Law [4]. While the capillary tube viscometer, the measuring instrument works using the principle of cohesion force, which cohesion is an attractive tensile force between similar molecules and in viscosity measurements has similar molecules [5]. The presence of solids however renders the determination of accurate and repeatable viscosity values into a haphazard endeavor [7]. Measurement of viscosity by rotational method depends on rotor movement to generate shearing motion, derive liquid viscosity through measuring the viscous torque of liquid on rotors or measuring the rotational speed of rotors. Rotational method can be further employed in the measurements of parameters, such as modulus and viscoelasticity of polymer materials [8-12].

In this research, researchers will design fluid viscosity measuring instruments with the rotary method or commonly known as a rotational viscometer. This research used rotation-type viscometers because this type of viscometer can accurately measure non-Newtonian fluid types compared to other types because it utilizes dc motor rpm to measure fluid viscosity values. This tool uses two sensors namely, rpm sensor to measure rpm of dc motor and current and voltage sensor to measure current from dc motor, and also use controller equipped with Internet of Things (IoT) so that the measurement results will be displayed through LCD and can be monitored through the website. This system will make it easier for the user to measure the fluid.

2. Method

2.1 Procedure

In this research, the outline of the research flow can be seen in Figure 1.

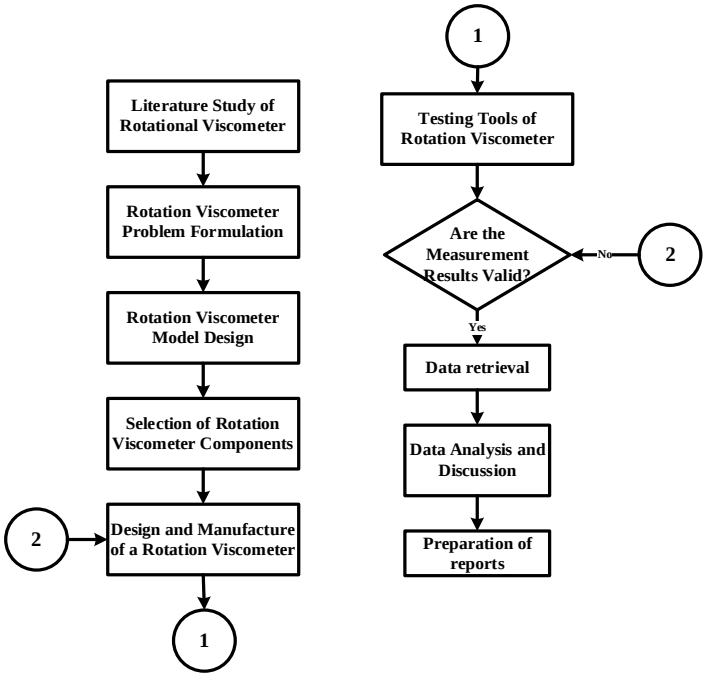

Fig. 1. Flowchart of Research Viscosity Measurement Tool

In the procedure of this research first, starting from literature research looking for references from journals and articles regarding the viscometer fluid measuring instrument using the rotary method based on the Internet of Things (IoT) or known as a rotational viscometer. Second, the problem formulation of the viscosity measuring instrument technology that is used and raised in this research is carried out. Third, making a model of the rotational viscometer which contains the design of the fluid viscometer. Fourth, the selection of components that will be used in making the rotational viscometer is carried out. Fifth, namely the design and manufacture of a fluid viscosity measuring instrument with a rotary method based on the Internet of Things (IoT). Sixth, a tool testing is carried out in which if the measurement results of the tool that have been made are invalid then it will do the design and remaking of the research tool, if it is in accordance with what is expected then the data is collected then the data will be analyzed and discussed on the data. The final step of this research is the preparation of a report on the results [15-17].

2.2 Design of Rotation Viscometer System Model

The system model in Figure 2 starts from the power supply that provides voltage to the DC motor and electrical circuit. When the DC motor works, the stirrer will move around stirring the liquid to be measured. Then the optocoupler sensor will sense the rpm of the DC motor and the reading value from the sensor will be sent to the controller. Likewise, with the INA219 sensor, this sensor will sense the current from the DC motor which then the readings from the sensor will be sent to the controller. Then the two sensor signals are processed by the controller. Then the results of the measurements can be seen through the LCD. In addition to the data displayed on the LCD, the data can also be viewed through the website, which controller will send data to the cloud.

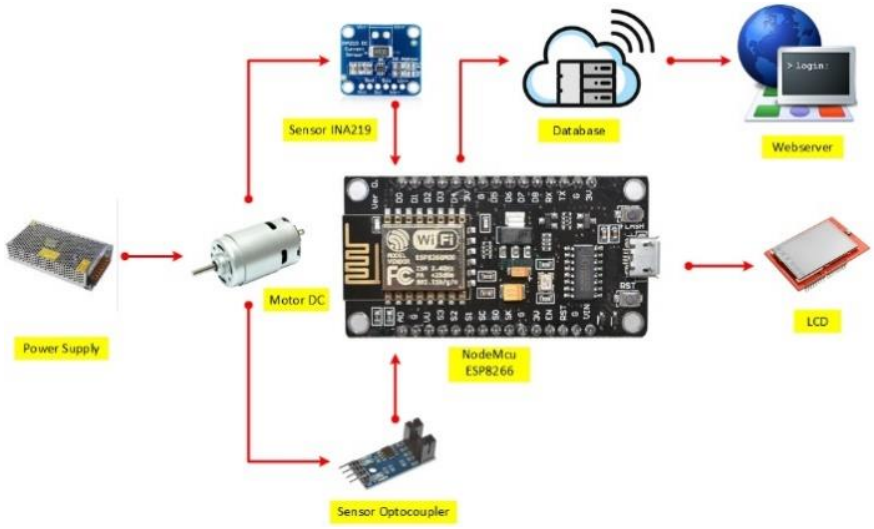

Fig. 2. Design of Rotation Viscometer System Model

2.3 Hardware and Software Design

Hardware design is divided into 2 groups, namely mechanical design and electronic device design. In the mechanical design there is a plant of a rotational viscometer. As for the electronic design, there are several components including a 12 Volt 3 Ampere DC power supply, step down circuit, 12 Volt DC Motor, FC 03 optocoupler sensor as a DC Motor speed sensor, INA219 sensor as a DC Motor current sensor, and NodeMCU LoLin V3 ESP8266 as a DC motor speed sensor. controllers. The LoLin V3 ESP8266 NodeMCU is in charge of receiving data from the speed sensor and current sensor for further processing and then the controller will send the data to the LCD for display and also to the webserver to be able to monitor the measurement results. In the software design system for the rotational method of fluid viscosity measuring instruments, several devices must be able to perform data retrieval, controller design, and data transmission. To be able to run it, this software design uses the Arduino IDE software.

2.3.1 Mechanical design

Figure 3 and Figure 4 are mechanical 3D designs of fluid viscosity measurement tools this design is made using SketchUp software. Figure 3 is a tool image in a closed box panel condition, and Figure 4 is the condition of an open box panel, where the image has several components in the panel box as described and numbered.

The following is the mechanical design scheme of liquid viscosity measuring instrument with a rotating method in 3D form:

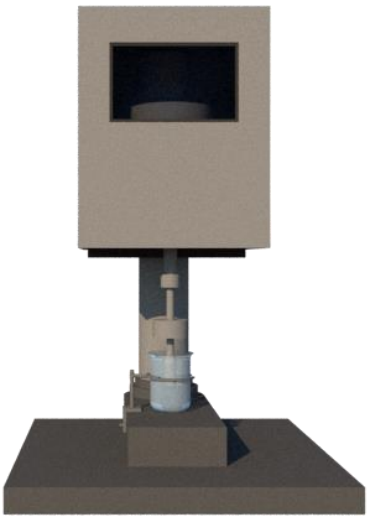

Fig. 3. Schematic of the 3d design of a fluid viscosity measuring instrument using the rotary method (a)

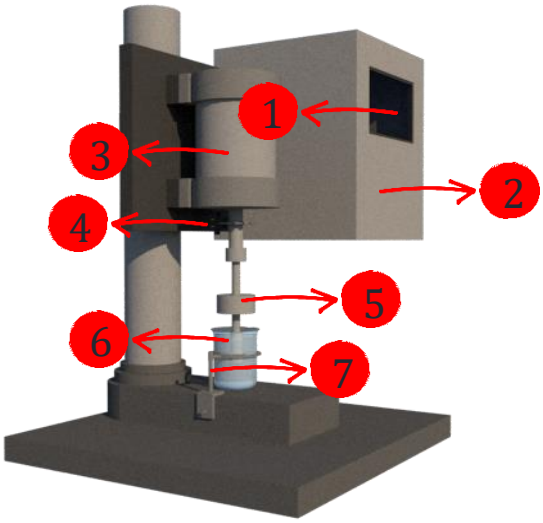

Fig. 4. Schematic of the 3D design of a fluid viscosity measuring instrument using the rotary method (b)

Information:

1) LCD
2) Panel
3) DC motor
4) Optocoupler sensor
5) Stirrer
6) Glass
7) Glass Handle

Figure 5 is the result of the realization of the 3D design of the fluid viscosity measurement tool. The measuring instrument can be adjusted the height of the panel box to make it easier to pour fluid to be measured into a beaker glass. The material used in this tool is, using cast iron on the base buffer and using stainless steel on some parts of the tool.

The following is the result of the realization of the mechanical design scheme of liquid viscosity measuring instrument with the rotary method:

Fig. 5. Mechanical Design Results

2.3.2 Electronic design

For electrical design in the form of wiring diagrams of fluid viscosity measuring instruments with IoT-based rotation method. Here is a wiring diagram of the fluid viscosity measuring instrument with IoT-based rotation method.

Figure 6 and Figure 7 are cable diagrams of fluid viscosity measurement tools. Figure 6 of the electrical diagram in the design using Visio software then Figure 7 is the result of the realization of the electrical diagram to be used in this research, the components used are NodeMCU ESP8266 as a controller, Power Supply 12V, LM2596 stepdown, INA219 sensor, Optocoupler sensor, 5V Relay, and DC 12V motor. The electrical will be placed on a panel box where one with the other has been integrated with each other.

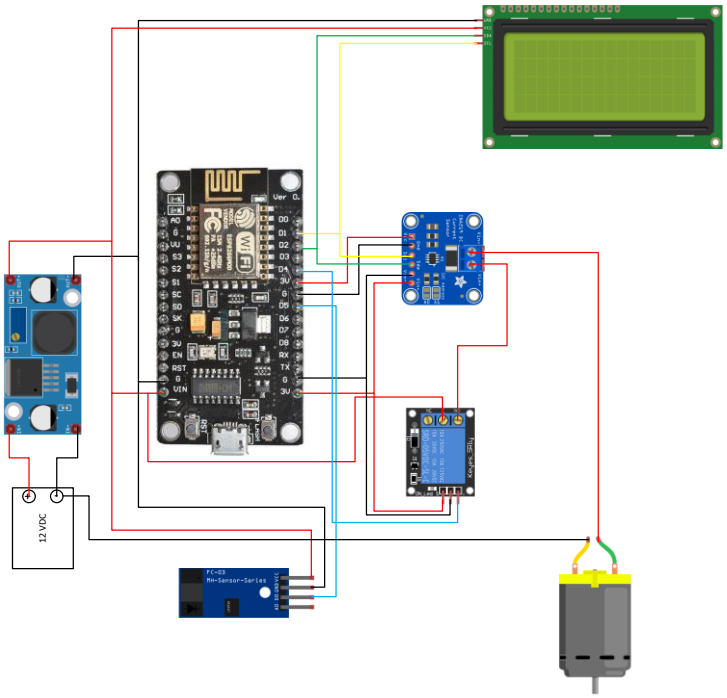

Fig. 6. Wiring Diagram

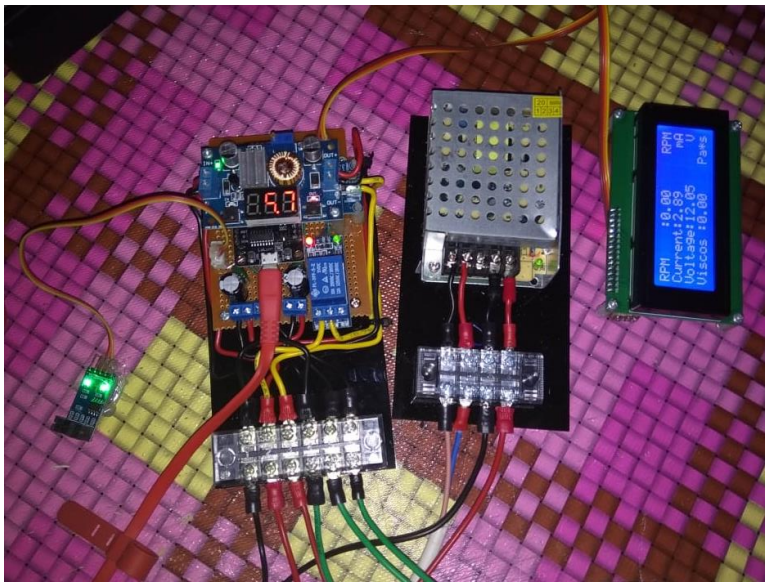

Fig. 7. Result of wiring diagram realization

2.3.2 NodeMCU software ESP8266

*NodeMcu ESP8266*used as the main microcontroller, which is used as a control between the sensor and the output for viscosity data. This ESP8266 NodeMCU functions as a data sender that connects the sensor to the plant. The data received from the INA219 sensor is in the form of analog data and the data received from the optocoupler sensor is digital data. So that the results of the readings of the two sensors will be processed by the controller which will produce viscosity data using the existing formula. As for the monitoring design for viscosity measurements using a webserver as follows:

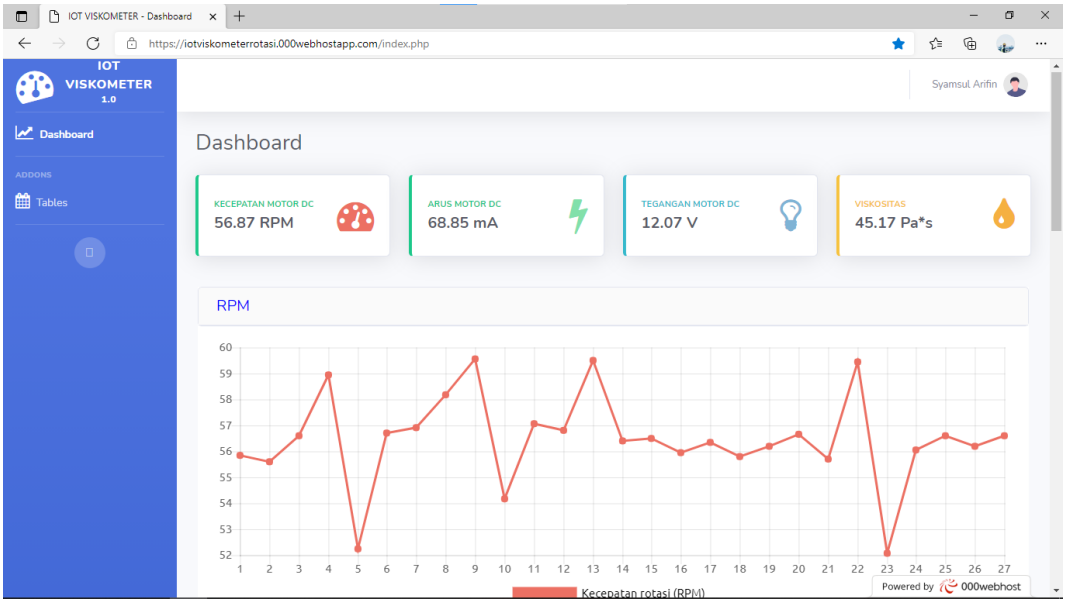

Fig. 8. Monitoring viscosity measurement using a webserver (a)

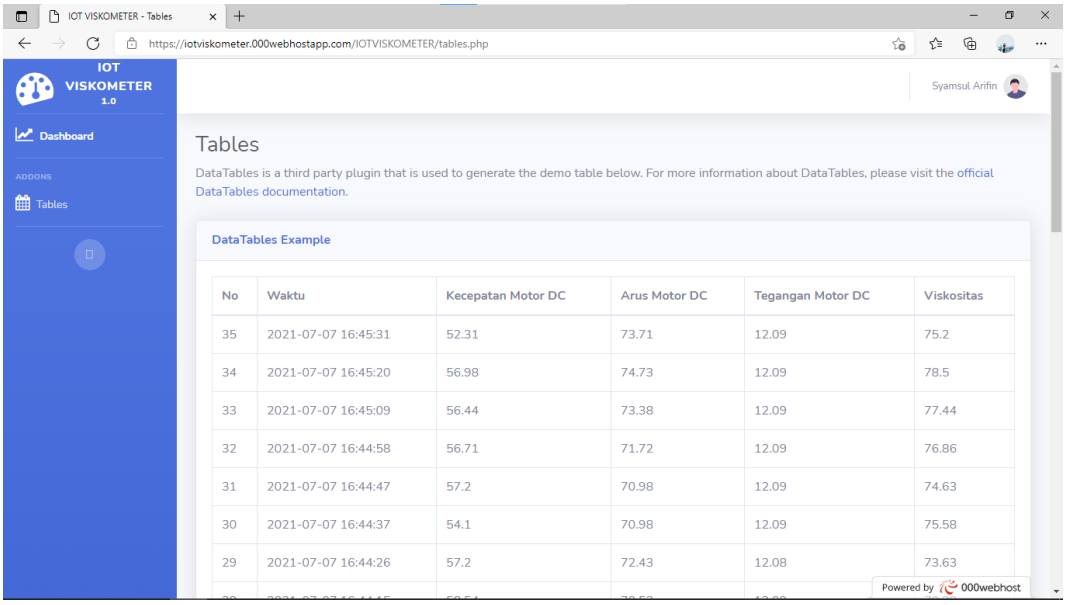

Fig. 9. Monitoring of viscosity measurement using a webserver (b)

Based on the image above, the measurement data can be monitored where on the webserver will display the results of measurement of dc motor current, rpm dc motor, and viscosity value results as in Figure 8. The webserver will also display graphs and tables of measurement results as in Figure 9. Monitoring can also be done anywhere can not only be done around the measuring instrument only.

3. Result and Discussion

3.1 Testing Each Component

Before the components are used to perform a function and are installed on the plant, we must be able to ensure whether the sensors or components that we install on the plant are working properly and the readings are in accordance with the readings of the tools that are considered standard.

3.1.1 Current and voltage sensor testing

In the fluid viscosity measuring plant, one of the variables measured is the current and voltage on the dc motor and monitored through the LCD and webserver. Before the sensor is assembled, the sensor must undergo testing and calibration first.

Figure 10 is a validation of the current sensor used in this research; validation is done by comparing the results of the current sensor with a standard current measuring device (multimeter). The image shows a result of 65.98 mA on the sensor reading and 66.8 mA on the multimeter reading, the result has been declared valid because the current sensor reading results are close to the results of multimeter readings.

Fig. 10. DC motor current test

Figure 11 is the validation of the voltage sensor used in the research. Similar to current sensors, this validation is done to compare voltage values by comparing the results of voltage sensors with standard voltage measuring instruments (multimeters). The image shows a result of 12.01 V on the sensor reading and 12.05 on the multimeter reading, the result of which has been declared valid because the voltage sensor reading results are close to the results of multimeter readings.

Fig. 11. DC motor voltage test

Sensor testing carried out is a fixed value test with a value of 60 mA at DC motor current and 12.02 V at DC motor voltage which refers to a multimeter validator. The steps are as follows:

(i) Setting up measuring instruments and multimeter validators
(ii) Attach the measuring instrument to be tested and the validator to the DC motor
(iii) Turn on the meter and validator at the same time
(iv) Read and record test results
(v) Repeat Steps c and d until you get the amount of data you want
(vi) Processing the data obtained from the test results to determine the feasibility level of the sensor

The following is the value of the current and voltage sensor test results with the current value on the DC motor.

Table 1 is the result of reading the current sensor and validator (multimeter). Validation was done ten times to ensure that the current sensor was properly viable for use in the research. From the results obtained in the table above it can be stated that the current sensor used in this research is suitable for use.

Table 1
Test results of current and voltage sensors on DC motor current values

No.	Tested Tool Readout "INA219 Sensor (mA)"	Validator Reading "Multimeter (mA)"	Correction	(X'-X)	(X'-X)^2
1	65.01	66.3	1.29	-0.624	0.389376
2	65.01	66.3	1.29	-0.624	0.389376
3	65.01	66.3	1.29	-0.624	0.389376
4	65.43	66.8	1.37	-0.204	0.041616
5	65.98	66.8	0.82	0.346	0.119716
6	65.98	66.8	0.82	0.346	0.119716
7	65.98	66.8	0.82	0.346	0.119716
8	65.98	66.8	0.82	0.346	0.119716
9	65.98	66.8	0.82	0.346	0.119716
10	65.98	66.8	0.82	0.346	0.119716

After testing, the characteristics of the current and voltage sensors will be obtained as follows:

Resolution	0.8	mA	
Average	64.634	mA	
Standard Deviation	0.462846267		
Validator Uncertainty	0.2	mA	
Level of confidence	95	%	
Coverage Factor	1.8		
Accuracy	1.4	%	
Standard Uncertainty	0.146364841		
Mathematical Models	66.65	±	0.616133
U1	0.146364841	mA	65.634
U2	0.180029759	mA	
Ub1	0.1	mA	
Ub2	0.230940108	mA	
Uc	0.342296238	mA	
U95	0.616133228		
veff	0.300871511		
Error Percentage	0.000152438	%	
Decision	The tool is still usable		

Table 2 is the result of the reading of the voltage sensor and validator (multimeter). Just like current sensors, voltage sensor validation was done ten times to ensure that the current sensor was properly viable for use in the research. From the results obtained in the table above it can be stated that the current sensor used in this research is suitable for use.

Table 2
Test results of current and voltage sensors on DC motor voltage values

No.	Tested Tool Readout "INA219 (V) Sensor"	Validator Reading "Multimeter (V)"	Correction	(X'-X)	(X'-X)^2
1	12	12.02	0.02	-0.006	3.6E-05
2	12	12.02	0.02	-0.006	3.6E-05
3	12.01	12.02	0.01	0.004	1.6E-05
4	12.02	12.05	0.03	0.014	0.000196
5	12.02	12.05	0.03	0.014	0.000196
6	12.01	12.02	0.01	0.004	1.6E-05
7	12.02	12.05	0.03	0.014	0.000196
8	12	12.02	0.02	-0.006	3.6E-05
9	12	12.02	0.02	-0.006	3.6E-05
10	11.98	12.01	0.03	-0.026	0.000676

After testing, the characteristics of the current and voltage sensors will be obtained as follows:

Resolution	0.8	V	
Average	12.006	V	
Standard Deviation	0.012649111		
Validator Uncertainty	0.2	V	
Level of confidence	95	%	
Coverage Factor	1.8		
Accuracy	0.5	%	
Standard Uncertainty	0.004		
Mathematical Models	12,028	±	0.453213
U1	0.004	V	12.006
U2	0.006804138	V	
Ub1	0.1	V	
Ub2	0.230940108	V	
Uc	0.2517848888	V	
U95	0.453212798	V	
veff	5.73276E-07		
Error Percentage	1.82907E-05	%	
Decision	The tool is still usable		

The following is the result of a comparison chart between the measuring instruments tested and the validator.

Figure 12 is a comparison graph of measuring instrument readings (current sensor) with a validator (multimeter) when testing each component for validation of the measuring instrument used. On the graph, the blue line is the result of a current sensor reading and the red line is the result of a multimeter reading. From the results of the current sensor test, the average current value is 65,634 mA which is close to the average value produced by the validator which is 66.65 mA.

Figure 13 is a comparison graph of measuring instrument readings (voltage sensor) with validator (multimeter) when testing each component for validation of the measuring instrument used. On the graph, the blue line is the result of a current sensor reading and the red line is the result of a multimeter reading. From the results of the current sensor test, the average current value is 12.006 V which is close to the value produced by the validator which is 12.028 V.

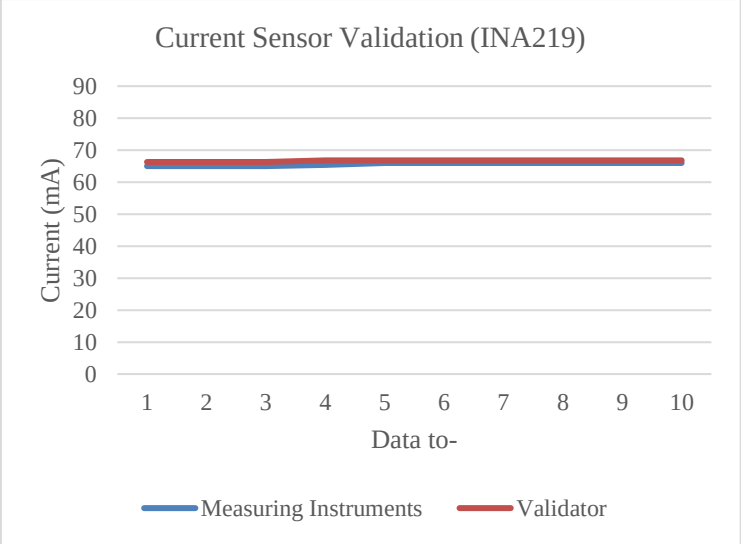

Fig. 12. Current Sensor Reading Results (INA219)

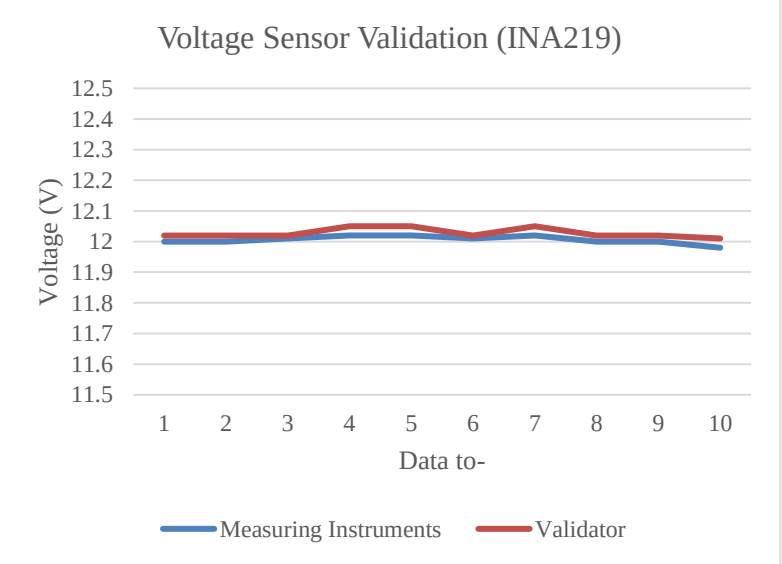

Fig. 13. Voltage Sensor Reading Results (INA219)

3.1.2 Speed sensor test

In this plant, a speed sensor is used to measure the speed of a dc motor. So that the results of this speed sensor will be monitored via the LCD and webserver. Before the sensor is assembled and installed in the plant, the sensor must be tested and calibrated first. In this speed sensor test, it is done using a tachometer as a comparison of the speed sensor in order to determine the level of accuracy and precision of the tool being tested. The results are as follows.

Figure 14 and Figure 15 are validation of the DC motor's rotary speed sensor. This validation is done using a tachometer. Validation is done to find out whether the sensor used is suitable for use or not. In Figure 14, the LCD shows the reading of the DC motor's rotary speed sensor of 56.87 rpm and Figure 15 shows a validator reading (tachometer) of 55.6 rpm. The results showed that the sensors used in the research were fit for use.

Fig. 14. Speed sensor test (optocoupler fc 03)

Fig. 15. Testing dc motor rpm with tachometer

Sensor testing carried out is a fixed value test carried out with a value of 59.2 rpm which refers to the tachometer validator. The steps are as follows:

(i) Setting up measuring instruments and tachometer validator
(ii) Attach the measuring instrument to be tested and the validator to the DC motor
(iii) Turn on the meter and validator at the same time
(iv) Read and record test results
(v) Repeat Steps c and d until you get the amount of data you want
(vi) Processing the data obtained from the test results to determine the feasibility level of the sensor

The following is the value of the speed sensor test results on a DC motor. Table 3 is the result of the reading of the rotary speed sensor and validator (tachometer). Just like current and voltage sensors, rotary speed sensor validation was done ten times to ensure that the sensor was fit for use in the research. From the results obtained in the table above it can be stated that the rotary speed sensor used in this research is suitable for use [18-21].

Table 3
Speed sensor test results

No.	Tested Tool Readout"FC 03 Optocoupler Sensor (rpm)"	Validator Reading "Tachometer (rpm)"	Correction	(X'-X)	(X'-X)^2
1	56.73	55.5	-1.23	-0.095	0.009025
2	56.73	55.5	-1.23	-0.095	0.009025
3	56.74	55.5	-1.24	-0.085	0.007225
4	56.87	55.6	-1.27	0.045	0.002025
5	56.87	55.6	-1.27	0.045	0.002025
6	56.87	55.6	-1.27	0.045	0.002025
7	56.87	55.6	-1.27	0.045	0.002025
8	56.87	55.6	-1.27	0.045	0.002025
9	56.85	55.6	-1.25	0.025	0.000625
10	56.85	55.6	-1.25	0.025	0.000625

After testing, the characteristics of the speed sensor will be obtained as follows:

Resolution	0.01	rpm	
Average	56.825	rpm	
Standard Deviation	0.063813966		
Validator Uncertainty	0.2	rpm	
Level of confidence	95	%	
Coverage Factor	1.8		
Accuracy	0.05	%	
Standard Uncertainty	0.020179748		
Mathematical Models	55.57	±	0.184404
U1	0.020179748	rpm	56.825
U2	0.008930952	rpm	
Ub1	0.1	rpm	
Ub2	0.002886751	rpm	
Uc	0.102446657	rpm	
U95	0.184403982		
veff	0.01354922	rpm	
Error Percentage	0.000225841	%	
Decision	The tool is still usable		

The following is the result of a comparison chart between the measuring instruments tested and the validator.

Figure 16 is a comparison graph of measuring instrument readings (rotary speed sensor) with a validator (tachometer) when testing each component for validation of the measuring instrument used. From the graph above the blue line is the result of sensor readings and the red lines are the result of tachometer readings. From the results of the current sensor test, the average current value is 56.825 rpm which is close to the value produced by the validator which is 55.57 rpm.

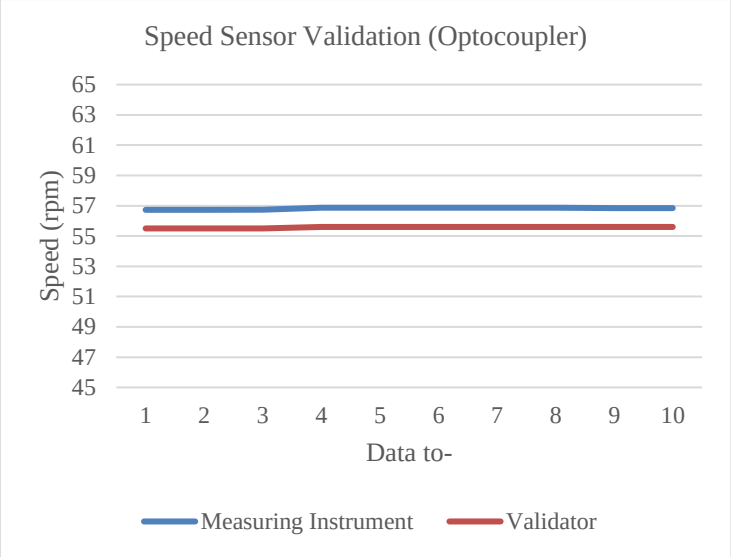

Fig. 16. Speed Sensor Reading Results

3.2 Fluid Viscosity Measuring Instrument Testing

Figure 17 is a viscosity measurement tool used in this research. After testing each component, it is done testing of fluid viscosity measuring instrument with a rotary method. The testing steps are as follows:

(i) Prepare oil for use as a sample on viscosity measurements
(ii) Plug the plug into a power outlet
(iii) Press the red push button to start viscosity measurement
(iv) Press the green push button to reset the fluid viscosity measurement readings when positioning without load or sample
(v) Perform Step a-d for another sample

Fig. 17. Fluid Viscosity Measuring Instrument

The following data of fluid viscosity measuring instrument test results using 3 samples, namely SAE 40 Oil, SAE 20W-50, and SAE 10W-30:

3.2.1 Testing with SAE 40 Oil samples

From testing using SAE 40 Oil obtained measurement results such as the following. Table 4 is the result of viscosity measurements using SAE 40 samples, measurements are made ten times with the aim of knowing the level of precision and accuracy of this research tool. The measurement results of this measuring instrument are also validated by calculating manually using the fluid viscosity formula. The results showed that in the SAE 40 sample, the accuracy rate obtained was 0.99.

Table 4
SAE 40 Oil Measurement Result Data

No.	Viscosity (Pa.s)		Correction	(X'-X)	(X'-X)^2
	Calculation	Measuring Instrument			
1	41.63	41.55	0.08	-34.674	1202.286
2	40.82	40.75	0.07	-35.474	1258.405
3	41.84	41.45	0.39	-34.774	1209.231
4	41.87	41.37	0.5	-34.854	1214.801
5	41.13	41.07	0.06	-35.154	1235.804
6	41.78	41.12	0.66	-35.104	1232.291
7	41.75	40.56	1.19	-35.664	1271.921
8	40.98	40.62	0.36	-35.604	1267.645
9	40.98	40.61	0.37	-35.614	1268.357
10	40.98	40.61	0.37	-35.614	1268.357
Average	41.376	40.971	0.405		1242.91
Standard Deviation					11.75164

Accuracy

$$= accuracy = \frac{100\%}{n}\sum_{t=1}^{n}\frac{|Xt-Pt|}{Xt}$$

$$= \left[1 - \left(\frac{(Average\ Standard\ Reading)-(Average\ Measuring\ Instrument)}{Average\ Standard\ Reading}\right)\right]$$

$$= \left[1 - \frac{41.376-40.971}{41.376}\right]$$

$$= 1 - (0.0097)$$

$$= 0.99$$

3.2.2 Testing with SAE 20W-50 Oil samples

From testing using SAE 20W-50 Oil obtained measurement results such as the following. Table 5 is the result of viscosity measurement using the SAE 20W-50 sample. Just like the first sample, measurements were made ten times with the aim of knowing the level of precision and accuracy of this research tool. The measurement results of this measuring instrument are also validated by calculating manually using the fluid viscosity formula. The results showed that in the SAE 20W-50 sample, the level of accuracy obtained was 0.99.

Table 5
SAE 20W-50 Oil Measurement Result Data

No.	Viscosity (Pa.s)		Correction	(X'-X)	(X'-X)^2
	Calculation	Measuring Instrument			
1	59.28	59.19	0.09	-53.886	2903.701
2	54.67	54.58	0.09	-58.496	3421.782
3	56.46	56.38	0.08	-56.696	3214.436
4	56.55	56.12	0.43	-56.956	3243.986
5	55.62	55.22	0.4	-57.856	3347.317
6	57.62	56.85	0.77	-56.226	3161.363
7	57.55	56.82	0.73	-56.256	3164.738
8	56.62	56.17	0.45	-56.906	3238.293
9	56.62	56.17	0.45	-56.906	3238.293
10	56.14	55.88	0.26	-57.196	3271.382
Average	56.713	56.338	0.375		3220.529
Standard Deviation					18.91657

Accuracy

$$= accuracy = \frac{100\%}{n}\sum_{t=1}^{n}\frac{|Xt-Pt|}{Xt}$$

$$= \left[1 - \left(\frac{(Average\ Standard\ Reading)-(Average\ Measuring\ Instrument)}{Average\ Standard\ Reading}\right)\right]$$

$$= [1 - \frac{56.713-56.338}{56.713}]$$

$$= 1 - (0.0066)$$

$$= 0.99$$

3.2.3 Testing with SAE 10W-30 Oil samples

From testing using SAE 10W-30 Oil, the measurement results are as follows. Table 6 is the result of viscosity measurement using the SAE 10W-30 sample. Just like the first and second samples, measurements were made ten times with the aim of knowing the level of precision and accuracy of this research tool. The measurement results of this measuring instrument are also validated by calculating manually using the fluid viscosity formula. The results showed that the SAE 10W-30 sample obtained an accuracy rate of 0.99.

Table 6
SAE 10W-30 Oil Measurement Result Data

No.	Viscosity (Pa.s)		Correction	(X'-X)	(X'-X)^2
	Calculation	Measuring Instruments			
1	68.06	67.96	0.1	-55.763	3109.512
2	66.95	66.85	0.1	-56.873	3234.538
3	67.15	66.75	0.4	-56.973	3245.923
4	66.34	66.03	0.31	-57.693	3328.482
5	65.99	65.12	0.87	-58.603	3434.312
6	66.12	65.95	0.17	-57.773	3337.72
7	67.68	66.85	0.83	-56.873	3234.538
8	67.39	66.42	0.97	-57.303	3283.634
9	67.39	66.42	0.97	-57.303	3283.634
10	67.02	66.22	0.8	-57.503	3306.595
Average	67.009	66.457	0.552		3279.889
Standard Deviation					19.0901

Accuracy

$$= accuracy = \frac{100\%}{n}\sum_{t=1}^{n}\frac{|Xt-Pt|}{Xt}$$

$$= \left[1 - \left(\frac{(Average\ Standard\ Reading)-(Average\ Measuring\ Instrument)}{Average\ Standard\ Reading}\right)\right]$$

$$= \left[1 - \frac{67.009-66.457}{67.009}\right]$$

$$= 1 - (0.0082)$$

$$= 0.99$$

3.3 Design Model

To facilitate in the analysis of the model that has been made, the model is made as shown in Figure 18.

Figure 18 is a model image of the design to be analyzed. The system consists of a series of mechanical and electronic components. The components consist of an electric motor integrated with the mixing drum. Between the mixing drum and the electric motor there is a shaft as a component to pass torque from the motor to the Drum.

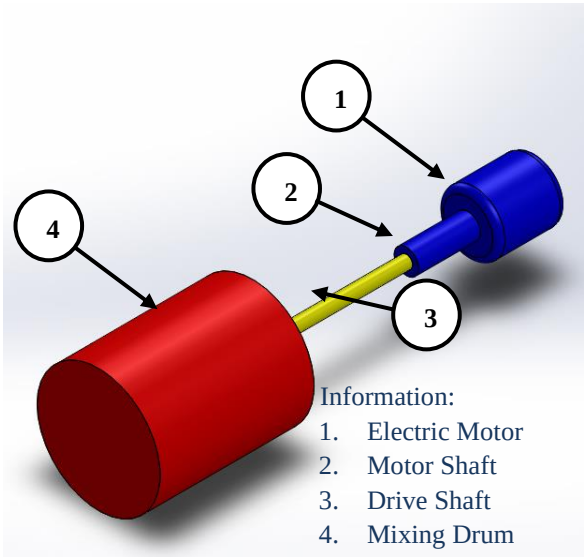

Fig. 18. Model of mixing drum integrated with motor

3.3.1 Model mathematics

To get a mathematical model of the system that has been designed as in Figure 18, then the image needs to be simplified to make it easier to get the mathematical model. The simplification of the image can be seen in Figure 19.

Figure 19 refers to the simplification components of a fluid viscosity gauge using a rotating drum. The system consists of an electric motor, motor shaft, drive shaft, and rotating drum that directly make contact with the test fluid. The analysis to get the mathematical model is as follows:

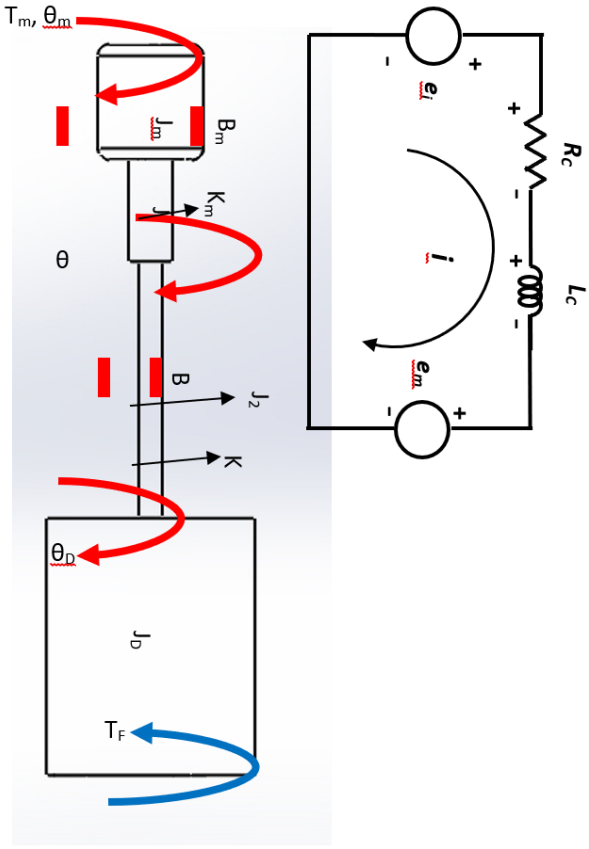

Fig. 19. Simplification of fluid viscosity measuring system using rotating drum

Information

T_m = torque from optimum engine (12 Nm at 320 rpm)
K_m = torque stiffness of the motor shaft
K = torque stiffness of the mixing shaft
B_m = motor damping coefficient
B = damping coefficient of the mixer shaft
ϑ_m = motor angle shift
ϑ = angle shift between clutch and shaft
ϑ_D = drum angle shift
J_m = moment of motor inertia
J = moment of motor shaft inertia
J_D = moment of drum inertia
T_F = shear voltage given fluid to the drum
e_m = induced voltage
L_C = conductor inductance
R_C = conductor resistance
R_L = obstacles in

Figure 20 and Figure 21 are diagrams of the drum drive motor. This system consists of a mechanical system (Figure 21) and an electrical system (Figure 20). In a mechanical system there is a motor torque obtained from electrical energy. This circuit consists of resistors, inductors, input voltage (from source) and mechanical stress to be converted into mechanical energy. The mechanical system of the motor consists of electric torque, shaft stiffness, moment of inertia, and motor

bearings. These components will later be used to find literature data and get a response from the motor.

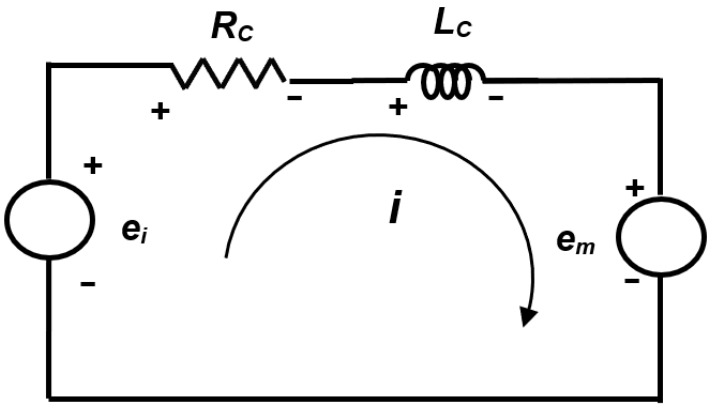

Fig. 20. Electrical Analysis [6]

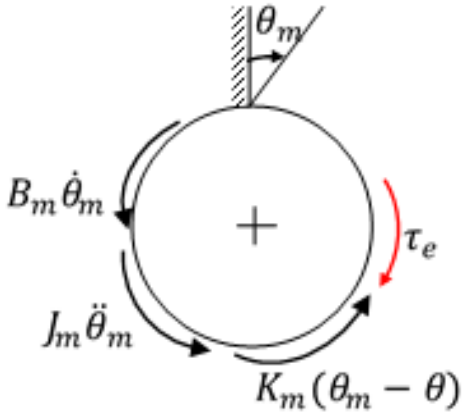

Fig. 21. FBD motor body

Figure 22 is a diagram of the drive shaft connecting the motor to the rotating drum. The function of this component is to transmit the torque of the motor rotation to the rotating drum. The components discussed in this analysis consist of the transmitted torque of the electric motor, the stiffness of the shaft and the moment of inertia of the mass of this shaft. This system is the link to the drum.

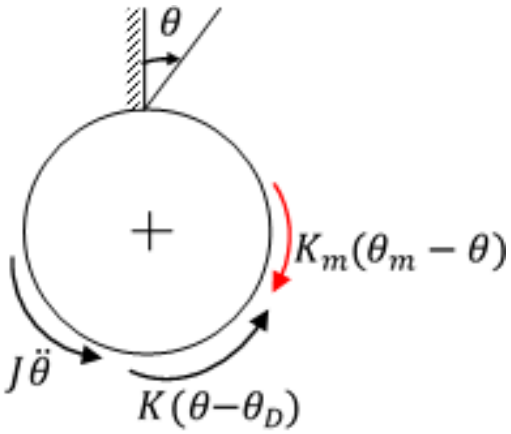

Fig. 22. FBD shaft body

Figure 23 is a diagrammatic image of a rotating drum. The components used in this simulation are the moment of inertia of the drum mass, the friction between the drum and the fluid and the magnitude of the intermediate shear stress applied to the drum by the fluid. The simulation results of this system will produce motor speed based on variations of fluid viscosity [14].

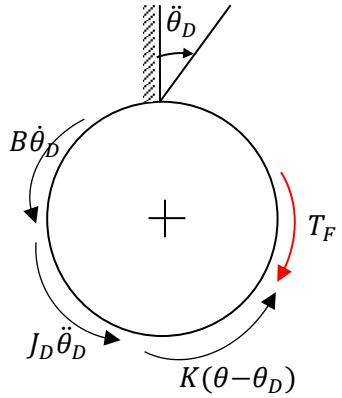

Fig. 23. FBD rotating drum body [6]

From FBD Above obtained Mathematical Equations

Electrical Analysis Results

$$e_i = iR_C + L_C\frac{di}{dt} + e_m \tag{1}$$

FBD Motor

$$\begin{aligned} &J_m\ddot{\theta}_m + B_m\dot{\theta}_m + K_m(\theta_m - \theta) = \tau_e \\ &\ddot{\theta}_m = \tfrac{1}{J_m}\left(\tau_e - B_m\dot{\theta}_m - K_m\theta_m + K_m\theta\right) \end{aligned} \tag{2}$$

FBD Shaft Body

$$\begin{aligned} &J\ddot{\theta} + K(\theta-\theta_D) = K_m(\theta_m - \theta) \\ &J\ddot{\theta} + K\theta - K\theta_D = K_m\theta_m - K_m\theta \\ &\ddot{\theta} = \tfrac{1}{J}(K_m\theta_m + K\theta_D - K_m\theta - K\theta) \end{aligned} \tag{3}$$

FBD drum

$$\begin{aligned} &J_D\ddot{\theta}_D + B_D\dot{\theta}_D + K(\theta_D - \theta) = T_F \\ &J_D\ddot{\theta}_D + B_D\dot{\theta}_D - K\theta + K\theta_D = T_F \\ &\ddot{\theta}_D = \tfrac{1}{J_D}\left(T_F - K\theta_D - B_D\dot{\theta}_D + K\theta\right) \end{aligned} \tag{4}$$

With $\dot{i} = \frac{di}{dt}$, $\tau_e = 2Nblri$ and $e_m = 2Nblr\dot{\theta}_m$, then the Eq. (3) is as follows

$$2Nblr\dot{\theta}_m = i_2 R_C + L_C \frac{di}{dt} + iR_L$$

From the Eq. (1), Eq. (2), Eq. (3) and Eq. (4), the state variable is obtained as follows

$$\begin{aligned}
&\omega_m = \dot{\theta}_m \\
&\dot{\omega}_m = \ddot{\theta}_m = \tfrac{1}{J_m}\left(2Nblri - B_m\dot{\theta}_m - K_m\theta_m + K_m\theta\right) \\
&\omega = \dot{\omega} \\
&\dot{\omega} = \ddot{\theta} = \tfrac{1}{J}(K_m\theta_m + K\theta_D - K_m\theta - K\theta) \\
&\omega_D = \dot{\theta}_D \\
&\dot{\omega}_D = \ddot{\theta}_D = \tfrac{1}{J_D}\left(T_F + K\theta_D - B_D\dot{\theta}_D - K\theta\right) \\
&\dot{i} = \tfrac{1}{L_c}\left(e_i - 2Nblr\dot{\theta}_m - iR_C\right)
\end{aligned} \tag{5}$$

3.3.2 Calculation of shaft torque rigidity and bearing friction coefficient

The amount of torque stiffness of the shaft can be done with the following equations

$$K = \frac{\pi.G.d^4}{32\ l} \tag{6}$$

where:
K = stiffness shaft (N/m)
G = sliding modulus (N/m2), the material used aluminum steel alloy, so large
G = 2.6 x 106 N/m2
l = length of motor shaft, l=0.02 m
d = diameter of motor shaft (m), d = 0.02 m
l = shaft length, l=0.05 m
d = shaft diameter (m), d = 0.01 m

So obtained the rigidity of the torque of the motor is

$$K_m = \frac{3{,}14x2{,}6x10^6x0{,}02^4}{32x0{,}02} = 2{,}041x10^{-4}kgm^2s^{-2}$$

While the rigidity of the shaft torque is

$$K = \frac{3{,}14x2{,}6x10^6x0.01^4}{32x0{,}05} = 5{,}1025x10^{-4}kgm^2s^{-2}$$

While the coefficient of friction of the bearing is as follows

$$B = \frac{2\pi\mu R^3 l}{d}$$

where:
B = attenuation coefficient (Ns/m)

μ = 0,3445
R = axis radius
l = length of the arm affected by friction
d = fluid height (0.1 mm)

From the data above, the attenuation coefficient value is obtained:

$$B_m = B = \frac{2.(3{,}14).(0{,}3445).(0{,}01)^3.(0{,}01)}{0{,}0001} = 0{,}00022\ Ns/m$$

3.3.3 Simulation results

Figure 24 is a Simulink block for fluid viscosity measuring system using rotating drum. These chart blocks are designed based on Eq. (1), Eq. (2), Eq. (3), Eq. (4), Eq. (5) and Eq. (6). The input of this system is an electric voltage of 5 Volts because the motor used is a DC electric motor with an input of 12 V. The simulation result of this system can be seen in Figure 25. From the results of this simulation obtained that initially the drum motor spins at a low speed until the 10th second of the motor rotation about 6 rad / s and as time increases, then the motor rotation will increase until the 60th second of the motor rotation begins to be constant this is due to the large shear voltage generated by the fluid at the beginning of the motor is turned on very large and decreases over time.

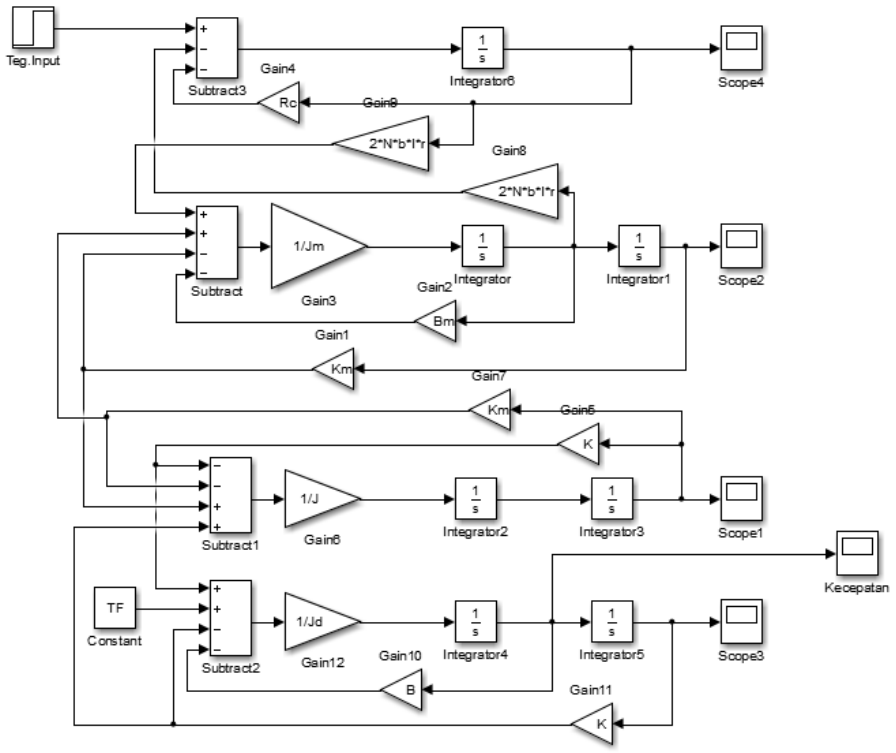

Fig. 24. Simulink block viscosity measuring system with electrical voltage input

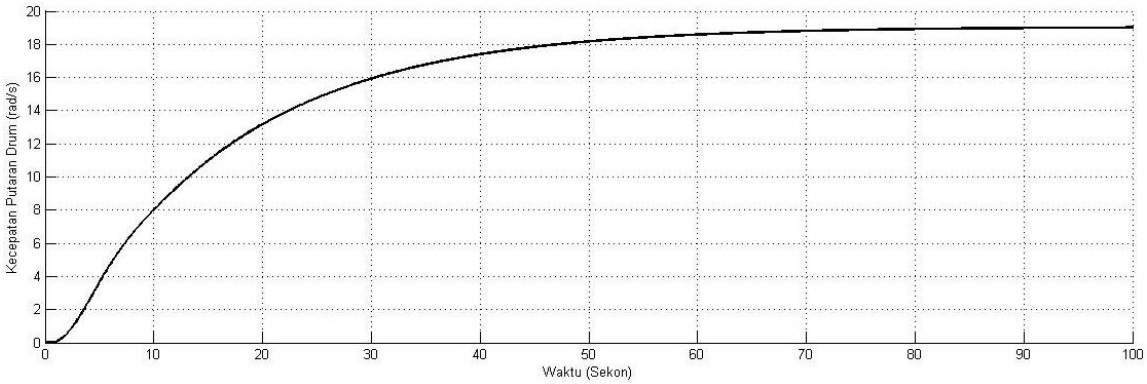

Fig. 25. Simulation result of fluid viscosity measuring instrument

4. Conclusion

The design of the fluid viscosity measuring instrument using the Internet of Things (IoT)-based rotary method was successfully created, starting from mechanical design, electrical design, and also a monitoring system using a webserver. SAE 40 Oil measurement results in the accuracy of 0.99, SAE 20W-50 Oil measurement obtained an accuracy value of 0.99, and in SAE 10W-30 Oil measurement obtained an accuracy value of 0.99. In addition to conducting research by conducting experiments using tools, this research is also carried out by conducting simulations using MATLAB software. From the simulation results, the drum motor rotates at a low speed until the 10th second of motor rotation is about 6 rad/s and with increasing time the motor rotation will increase until the 60th second the motor rotation starts to remain constant this is due to the large shear stress generated by the fluid at the start of the motor is very large and decreases with time.

Acknowledgment

The authors gratefully acknowledge financial support from the Institut Teknologi Sepuluh Nopember for this work, under project scheme of the Publication Writing and IPR Incentive Program (PPHKI).

References

[1] Firmansyah, Rizqi Rindra, and Imam Sucahyo. "Rancang bangun viskometer rotasi sebagai pengukur kekentalan fluida cair." *Inovasi Fisika Indonesia* 8, no. 2 (2019).

[2] IBS. "Ketahui Lebih Banyak Manfaat Rumus Viskositas." *Infinity Bioanalitika Solusindo*. March 19, 2019. https://ibs.co.id/id/rumus-viskositas/.

[3] Samdara, Rida, Syamsul Bahri, and Ahmad Muqorobin. "Rancang Bangun Viskometer Dengan Metode Rotasi Berbasis Komputer." *GRADIEN: Jurnal Ilmiah MIPA* 4, no. 2 (2008): 342-348.

[4] Putri, Bias ML, Sissilia O. Putri, Farida I. Muchtadi, and Faqihza Mukhlish. "Pembuatan Prototipe Viskometer Bola Jatuh Menggunakan Sensor Magnet dan Bola Magnet." *Jurnal Otomasi, Kontrol & Instrumentasi* 5, no. 2 (2015): 101-111. https://doi.org/10.5614/joki.2013.5.2.6

[5] Mulyana, Rachmat. "Pengukuran Viskositas Air Memakai Pipa Kapiler Dengan Metode Poiseuille." *Fakultas Matematika dan Ilmu Pengetahuan Alam, Universita Indonesia* (2009).

[6] Sampurno, Bambang, Arief Abdurrakhman, and Herry Sufyan Hadi. "Development of electrical Kinetic Energy Recovery System (KERS) on motorcyle." In *2015 International Conference on Advanced Mechatronics, Intelligent Manufacture, and Industrial Automation (ICAMIMIA)*, pp. 131-136. IEEE, 2015. https://doi.org/10.1109/ICAMIMIA.2015.7508017

[7] Wang, Yannan, Zhuangzhuang Liu, Lingling Cao, Bart Blanpain, and Muxing Guo. "Simulation of particle migration during viscosity measurement of solid-bearing slag using a spindle rotational type viscometer." *Chemical Engineering Science* 207 (2019): 172-180. https://doi.org/10.1016/j.ces.2019.06.022

[8] Ramos, Pedro M., Fernando M. Janeiro, and Pedro S. Girão. "Uncertainty evaluation of multivariate quantities: A case study on electrical impedance." *Measurement* 78 (2016): 397-411. https://doi.org/10.1016/j.measurement.2015.08.043

[9] McGregor, Robert, and Jodi Armstrong. "Viscosity Analysis: Flow Curve, Yield Stress and Creep." *Adhesive and Sealants Industry*. October 1, 2015. https://www.adhesivesmag.com/articles/94189-viscosity-analysis-flow-curve-yield-stress-and-creep.

[10] Hajikarimi, Pouria, Mohammad Rahi, and Fereidoon Moghadas Nejad. "Comparing different rutting specification parameters using high temperature characteristics of rubber-modified asphalt binders." *Road Materials and Pavement Design* 16, no. 4 (2015): 751-766. https://doi.org/10.1080/14680629.2015.1063533

[11] Yousefi Kebria, Daryoush, S. Rohalah Moafimadani, and Yaser Goli. "Laboratory investigation of the effect of crumb rubber on the characteristics and rheological behaviour of asphalt binder." *Road Materials and Pavement Design* 16, no. 4 (2015): 946-956. https://doi.org/10.1080/14680629.2015.1042015

[12] Serbezeanu, Diana, Ana Maria Popa, Timea Stelzig, Ion Sava, Rene M. Rossi, and Giuseppino Fortunato. "Preparation and characterization of thermally stable polyimide membranes by electrospinning for protective clothing applications." *Textile Research Journal* 85, no. 17 (2015): 1763-1775. https://doi.org/10.1177/0040517515576326

[13] de Castro, Claudia Santos Cardoso, Dalni Malta do Espírito Santo Filho, José Renato Real Siqueira, Alex Pablo Ferreira Barbosa, Claudio Roberto da Costa Rodrigues, Maurício Limp Cabral, Evelyn Meireles da Silva, Felipe de Oliveira Baldner, and José Maurício Gomes Gouveia. "Evaluation of the metrological performance of two kinds of rotational viscometers by means of viscosity reference materials." *Journal of Petroleum Science and Engineering* 138 (2016): 292-297. https://doi.org/10.1016/j.petrol.2015.12.003

[14] Hadi, Herry Sufyan, Arief Abdurrakhman, Ahmad Fauzan Adziimaa, Brian Rafiu, Murry Raditya, Mohammad Berel Toriki, Sefi Novendra Patrialova, Harsono Hadi, and Dwi Oktavianto W. Nugroho. "Design and Simulation of Herbal Medicine Milling System." In *2019 International Conference on Advanced Mechatronics, Intelligent Manufacture and Industrial Automation (ICAMIMIA)*, pp. 155-158. IEEE, 2019. https://doi.org/10.1109/ICAMIMIA47173.2019.9223408

[15] Ma, Quanjin, M. R. M. Rejab, Bo Sun, and M. N. M. Merzuk. "A brief review of the cubic star on structural design, applications, and future perspective." *Journal of Advanced Research in Applied Sciences and Engineering Technology* 24, no. 1 (2021): 10-17. https://doi.org/10.37934/araset.24.1.1017

[16] Lubis, Hamzah. "Renewable Energy of Rice Husk for Reducing Fossil Energy in Indonesia." *Journal of Advanced Research in Applied Sciences and Engineering Technology* 11, no. 1 (2018): 17-22.

[17] Wee, Choo Chee, Muralindran Mariappan, Resot Iggau, Brendan Khoo, and Wong Wei Kitt. "Circuit design and development of contactless sensor system for finger tracking in piano playing." *Journal of Advanced Research in Applied Sciences and Engineering Technology* 5, no. 2 (2016): 46-54.

[18] Salbi, Noorsabrina M., Norhayati Muhammad, and Norazlin Abdullah. "The Effect of Maltodextrin and Acacia Gum on Encapsulation of Fig Powder Physicochemical Properties." *Journal of Advanced Research in Applied Sciences and Engineering Technology* 22, no. 1 (2021): 8-15. https://doi.org/10.37934/araset.22.1.815

[19] Yahya, Noor Fateen Afikah, Negar Dasineh Khiavi, and Norahim Ibrahim. "Green electricity production by Epipremnum Aureum and bacteria in plant microbial fuel cell." *Journal of Advanced Research in Applied Sciences and Engineering Technology* 5, no. 1 (2016): 22-31.

[20] Khalid, Hasmawi, and Norhayati Ibrahim. "Charphy Impact of Medium Molecular Weight Phenol Formaldehyde (MMwPF) Plywood." *Journal of Advanced Research in Applied Sciences and Engineering Technology* 18, no. 1 (2020): 24-30. https://doi.org/10.37934/araset.18.1.2430

[21] Aziz, Ameera Syaheerah Abdul, Nurul Syahirah Mohamad Nasir, Norahim Ibrahim, and Adibah Yahya. "Decolorization of Azo Dye AR27 and bioelectricity generation in microbial fuel cell." *Journal of Advanced Research in Applied Sciences and Engineering Technology* 5, no. 1 (2016): 32-41.